Int J Clin Exp Med 2020;13(12):9318-9330
www.ijcem.com /ISSN:1940-5901/IJCEM0120679

Original Article

Effect of miR-132-3P targeted high-mobility group AT-Hook 2 on vascular endothelial growth factor signaling pathway and serum bone markers during fracture healing in rats

Qiang Fu[1,2], Jian Wang[2], Hui Zhao[2], Zaijun Wang[2], Weiguo Liang[1]

[1]*Department of Orthopedics, Guangzhou Red Cross Hospital, Medical College, Ji'nan University, Guangzhou, Guangdong Province, China;* [2]*Department of Orthopedics, The First Affiliated Hospital of Jinzhou Medical University, Jinzhou, Liaoning Province, China*

Received August 19, 2020; Accepted September 16, 2020; Epub December 15, 2020; Published December 30, 2020

Abstract: Objective: We hypothesized that miR-132-3P could target HMGA2 to affect vascular endothelial growth factor (VEGF) signaling pathway and serum bone markers during fracture healing in rats. Methods: The targeting relationship between miR-132-3p and HMGA2 was verified by dual luciferase reporter assay. After the overexpression of miR-132-3p or the knockdown of HMGA2 in bone fracture rats, the levels of procollagen type 1 N-terminal propeptide, bone alkaline phosphatase and osteocalcin were significantly increased; the HMGA2 gene expression level was significantly decreased; the VEGF and bone morphogenetic protein 2 gene expression levels were significantly elevated. Results: Trabecular bone remodeling was in relatively high speed and fracture healing in rats was simultaneously promoted. In miR-132-3p mimic + siRNA-HMGA2 group, the aforementioned effects were enhanced. Conclusion: miR-132-3p could target and regulate the expression of HMGA2, activate VEGF signaling pathway, improve the levels of bone markers, and thus promote fracture healing in rats.

Keywords: miR-132, HMGA2, fracture healing, vascular endothelial growth factor

Introduction

Bone fracture refers to continuous complete or partial break of the bone structure, and often clinically occurs in orthopedics [1]. Children and the elderly are the main vulnerable population, and fractures still exist among young and middle-aged people [2]. A bone fracture might be caused by direct or indirect strong stress or cumulative strain. Severe pain is the most prominent symptom presenting in patients with ongoing fracture; a severe case will cause necrosis in the fracture site and thus trigger neurological dysfunction if not treated in time [3-5]. Therefore, strong attention should be paid to the fracture healing.

Fracture healing is a complex, highly regulated biological process that involves a variety of cytokines and gene expression [6]. MicroRNAs (miRs) are non-coding single-stranded RNA molecules that play important roles in regulating cell proliferation, apoptosis, migration, and differentiation after binding with target mRNAs [7, 8]. MicroRNAs such as miR-26a, miR-133, miR-135, miR-29, miR-141 and iniR-200a have been proved to be closely related to bone formation [9-12]. MiR-132, located on chromosome 17 of the human body, consists of two homologous miRNAs (hsa-miR-132-5p, hsa-miR-132-3p). It has been studied in many tissues and diseases, such as osteosarcoma, neural cell differentiation, and inflammation [13]. Moreover, miR-132, as one of endothelial cell-specific miRNAs, plays an important role in angiogenesis by acting on stimulating factor of neovascularization [14]. And it is well known that microRNA mainly acts by binding to target genes. As a result, we in this study explore for the first time that high-mobility group protein AT-hook 2 (HMGA2) is a potential target gene of miR-132-3p.

HMGA2 is a non-histone chromosomal high-mobility group protein, which may play an important role in promoting epithelial-mesenchymal transformation and maintaining the differentiation potential and self-renewal ability of stem cells. Furthermore, the vascular endothelial growth factor (VEGF) pathway is closely related to the role of HMGA2, which was one of many signaling pathways that HMGA2 participates in biological processes in vivo. Reversely, HMGA2 indirectly regulates the expression of VEGF and other proteins by increasing the activity of the transcription factor activator protein 1 (AP1) complex.

VEGF has become the focus of research, as it has a strong effect on angiogenesis. Moreover, angiogenesis is an important biological part for fracture repair. As a result, VEGF is considered to play an essential role in the process of bone formation and fracture healing [15]. A study found that VEGF was positively expressed in the whole process of fracture healing, and the expression peak of VEGF presented at day 7 to 28 after fracture, which was highly consistent with the vascular reconstruction stage in the process of tissue healing [16].

This article explores the role of miR-132-3p combined with VEGF in fracture healing for the first time, hoping to bring up a new way for the treatment of bone fracture, thereby benefiting the majority of fracture patients.

Methods and materials

Animal modeling

A total of 115 8-week-old healthy male Sprague-Dawley rats weighing 180 g to 220 g were provided by the Laboratory Animal Research Center of Guangzhou University of Traditional Chinese Medicine. The rats were caged in a temperature-controlled room at 25°C, fed standard rat chow diet and water ad libitum, allowed unrestricted movement for two weeks of adaptive rearing before the experiment. Fifteen rats were randomly selected as Normal group, and the rest were used for fracture modeling [17]. The rest rats were intraperitoneally injected with 2% phenobarbital sodium (30 mg/kg; H31020502, Shanghai New Asia Pharmaceutical Co., Ltd., China) for anesthesia. The knees were then bent at 90 degrees and fixed in supine position, and then longitudinal incision (about 1 cm) was made at the patella of the left knee joint. The tendinous tissue of the quadriceps femoris and joint capsule were cut open along the medial edge of the patella, followed by further slowly bending the knee joint. After turning the patella outward, a stainless-steel needle was inserted into the bone marrow, with the shank snipped off and needle end buried in the intercondylar fossa of femur. When the activity of knee joint is unaffected, the incision was sutured layer by layer. The treated rats were placed in supine position with the left thigh on an impact table, and a weight of 300 g was dropped from a height of 20 cm for establishing femoral fracture. After successful modeling, the rats were reared and fed in the aforementioned way. This study was approved by the Animal Ethics Committee of the First Affiliated Hospital of Jinzhou Medical University, and the rats were treated according to the national principles of laboratory animal care and management.

Animal grouping

The 50 nmol/L miR-132-3p mimic plasmid, mir-132-3p inhibitor plasmid, and siRNA-HMGA2 were rapidly centrifuged, respectively, followed by homogenization with 170 μL phosphate buffered saline (PBS) each and standing for 5 min. Then 30 μL Lipofectamine™ 2000 transfection reagents were added into the three mixtures, with standing for 20 min. Thus, three liposome complexes were prepared for later use. Plasmids used in the study were all obtained from Shanghai GenePharma Co., Ltd., China.

The 15 normal rats without bone fracture were taken as Normal group. Ninety model rats were randomly divided into six groups: model group (without any treatment), negative control (NC) group (injected with 200 μL miR-132-3p negative-control liposome complex), miR-132-3p mimic group (injected with 200 μL miR-132-3p mimic liposome complex), miR-132-3p inhibitor group (injected with 200 μL miR-132-3 inhibitor liposome complex), siRNA-HMGA2 group (injected with 200 μL siRNA-HMGA2 liposome complex), and miR-132-3p mimic + siRNA-HMGA2 group (injected with both miR-132-3p mimic and siRNA-HMGA2 liposome complexes), with 15 rats in each group. All the model rats received injection via caudal vein once a day for three consecutive days.

Sample collection

At the 2nd, 4th and 8th weeks after modeling, five rats in each group were randomly selected at each time. After 12-hour fasting, 5 mL of blood sample through caudal vein was taken from each rat, with standing at room temperature for 2 h. Then the blood was centrifuged at 4°C, 1,000 g for 15 min; the upper layer was pipetted out and stored at -80°C for subsequent ELISA detection. After that, the rats were anesthetized and sacrificed, followed by rapid removal of left femur head. The obtained femur head was fixed in 10% formaldehyde solution for 24 h, and decalcified in 10% ethylenediamine tetra-acetic acid (CAS: 60-00-4; Beijing Zhongshan Golden Bridge Biotechnology Co., Ltd., China) solution for three weeks (the solution was changed every 5 days), then embedded in paraffin, and stored at -20°C for subsequent HE staining and immunohistochemical analysis. The right femur heads of rats were taken with cartilaginous tissue removed, and then stored at -80°C for subsequent quantitative reverse transcription polymerase chain reaction (qRT-PCR) and Western blotting.

Bioinformatics analysis and dual-luciferase reporter gene assay

The target gene of miR-132-3p was analyzed using the biological prediction website, Targetscan.org. And dual-luciferase reporter gene assay was used to verify whether HMGA2 was the direct target gene of miR-132-3p. The full length of 3'-untranslated region (UTR) of HMGA2 gene was cloned and amplified. The polymerase chain reaction (PCR) product was cloned into the multiple cloning sites in the downstream of the luciferase gene to the pmirGLO (E1330; Promega Corporation, Madison, WI, USA). Bioinformatics analysis software was utilized to predict the binding sites of miR-132-3p on target gene, and site-directed mutagenesis was then carried out to construct the wild-type strain (HMGA2-Wt) harboring the luciferase reporter plasmid with target site in 3'UTR of HMGA2. And point mutation of complementary site of 3'UTR of HMGA2 and miR-132-3p was carried out for constructing luciferase plasmid containing S mutation sequence (HMGA2-Mut), with pRL-TK vector (TaKara Bio Company, USA) expressing Renilla luciferase as the internal control. HEK-293T cells (Cell Resource Center of the Shanghai Institutes for Biological Sciences of the Chinese Academy of Sciences) were cultured in a 24-well plate; and when the cell confluence reached 80% to 90%, correctly sequenced luciferase reporter plasmids, HMGA2-Wt and HMGA2-Mut were co-transfected with miR-132-3p NC and miR-132-3p mimic, respectively, into HEK-293T cells. Dual-luciferase reporter gene assay was conducted according to the operations provided by Promega.

ELISA

The levels of serum bone markers, procollagen type 1 N-terminal propeptide (P1NP), bone alkaline phosphatase (BAP) and osteocalcin (OC) in all rats were determined by ELISA. All determinations for the serum P1NP, BAP and OC levels were carried out according to the instructions of the corresponding ELISA kits (Wuhan Huamei Biotech Co., Ltd., China). After the determinations, the optical density (OD) at 450 nm of each well was read by the Bio-Tek™ Synergy™ 2 multi-mode microplate reader (USA). The standard curve was drawn with the concentration of standard as abscissa and the OD value as ordinate.

Hematoxylin and eosin staining

Paraffin sections of femoral tissues in each group were taken continuously at a thickness of 5 μm, and incubated at 60°C overnight, followed by conventional dewaxing, hydration, and rinsing with distilled water twice, 2 min each time. Then the sections were dyed with hematoxylin (Shanghai Bogoo Biotechnology Co., Ltd., China) for 3 min, rinsed with tap water, placed in ethanol solution containing 1% hydrochloric acid for 5 s, and rinsed with tap water until the sections changed to blue. After that, the sections were dyed with eosin (Shanghai Bogoo Biotechnology Co., Ltd., China) for 5 min, followed by conventional gradient alcohol dehydration, and sealed by neutral resin. Callus thickness and maturity were measured under Olympus microscope (Shanghai Fairy Optical Technology Co., Ltd., China).

Immunohistochemical assay

Paraffin sections of femur heads of rats were taken continuously at 5 μm thickness. After conventional slice-baking, dewaxing, hydration, and antigen retrieval, sections were incubated

Table 1. List of primer sequences for quantitative reverse transcription polymerase chain reaction

Genes	Primer sequences
miR-132-3p	Forward: 5'-ACACTCCAGCTGGGTAACAGTCTACAG-3'
	Reverse: 5'-CTCAACTGGTGTCGTGGA-3'
HMGA2	Forward: 5'-CCAAACGTGCTGGGCAGCTCCGG-3'
	Reverse: 5'-CCCCTCTTGATTCCTAGGTCT-3'
VEGF	Forward: 5'-ACCAGCGCAGCTATTGCCGT-3'
	Reverse: 5'-CGCCTTGGCTTGTCACA-3'
BMP-2	Forward: 5'-GATTGACTCCATTGGCCCTA-3'
	Reverse: 5'-GGCTAGTTTCTGGGCAGTTG-3'
U6	Forward: 5'-GGTCGGGCAGGAAAGAGGGC-3'
	Reverse: 5'-GCTAATCTTCTCTGTATCGTTCC-3'
GADPH	Forward: 5'-GTTTCTTACTCCTTGGAGGCCAT-3'
	Reverse: 5'-TGATGACATCAAGAAGTGGTGAA-3'

Note: HMGA2: high-mobility group AT-hook 2; VEGF: vascular endothelial growth factor; BMP-2: bone morphogenetic protein-2; GADPH: glyceraldehyde-3-phosphate dehydrogenase.

with 5% hydrogen peroxide for 20 min, and sealed with 5% normal goat serum for 1 h. Then the sections were incubated with rabbit anti-mouse HMGA2 primary antibody (1:1,000; Abcam, UK) overnight at 4°C, followed by incubation with goat anti-rabbit IgG (1:2,000; Abcam, UK) at 37°C for 1 h, and then with diaminobenzidine solution (Sigma Corporation, USA) for 4 to 5 min at room temperature in a dark place. After the incubations, the sections were counterstained with hematoxylin (Shanghai Bogoo Biotechnology Co., Ltd., China) for 3 min, followed by conventional dehydration to transparency, and sealed by neutral resin. The treated sections were visualized by Olympus microscope (Shanghai Fairy Optical Technology Co., Ltd., China). PBS was used in the immunohistochemical assay instead of primary antibody for negative control. The positive expression rate of HMGA2 was determined by the depth and quantity of positive staining. Cytoplasm or nucleus stained yellow brown indicated positive expression.

Quantitative reverse transcription PCR

Total RNA was extracted from fracture tissues in each group by RNA extraction kit (Invitrogen Company, United States). Primers were designed by Primer Premier 5.0, and synthesized by Shanghai Sangon Biotech Co., Ltd., China. The primer sequences are shown in **Table 1**. Then the RNA was reversely transcribed into cDNA using PrimeScript RT kit (TaKaRa, Japan). The volume of reverse transcription system was 10 μL, and the reaction mixture were incubated at 70°C for 5 min, followed by ice bath for 2 min, and incubation at 42°C for 50 min and 70°C for 8 min. The cDNA was temporarily stored at -80°C. The operations of quantitative fluorescence PCR were carried out according to the instructions of SYBR® Premix Ex Taq™ II kit (TaKaRa, Japan) using Bio-Rad iQ™5 Real-Time PCR Detection System (Bio-Rad, Hercules, CA, USA). The reaction conditions were as follows: pre-denaturation at 95°C for 30 s, followed by 40 cycles of denaturation at 95°C for 10 s, annealing at 60°C for 20 s, and lastly extension at 70°C for 10 s. The internal control gene for miR-132-3p was U6, and that of HMGA2, VEGF and bone morphogenetic protein-2 (BMP-2) was glyceraldehyde-3-phosphate dehydrogenase (GADPH), and the expression levels of miR-132-3p, HMGA2, VEGF and BMP-2 were calculated by $2^{-\Delta\Delta Ct}$ method.

Western blotting

The right femur heads of rats prepared before were pulverized in liquid nitrogen, then ground into homogenate on ice after addition of 1 mL tissue lysis buffer (Beijing Solarbio Science & Technology Co., Ltd., China), followed by lysis at 4°C for 30 min with protein lysis buffer (Shanghai Beyotime Biotechnology Co., Ltd., China). After centrifugation at 10,000 g and 4°C for 20 min, the supernatant was collected. The protein concentration in each sample was determined according to the instructions of QuantiPro™ BCA Assay Kit (Sigma, USA) for protein. After bathing in water at 100°C for 10 min for lysis, the supernatant samples were pipetted into wells, and the total proteins were electrophoretically separated in 10% sodium dodecyl sulfate (SDS)-polyacrylamide gel (Shanghai Chem Biomedical Co., Ltd., China), and after 120 min the samples were transferred from the gel to nitrocellulose membrane. The membrane was then immersed in 1×TBST (a mixture of tris-buffered saline and Polysorbate 20) buffer containing 5% skimmed milk powder and gently shaken at room temperature for 1 h. After being sealed, the membrane was rinsed with TBST 3

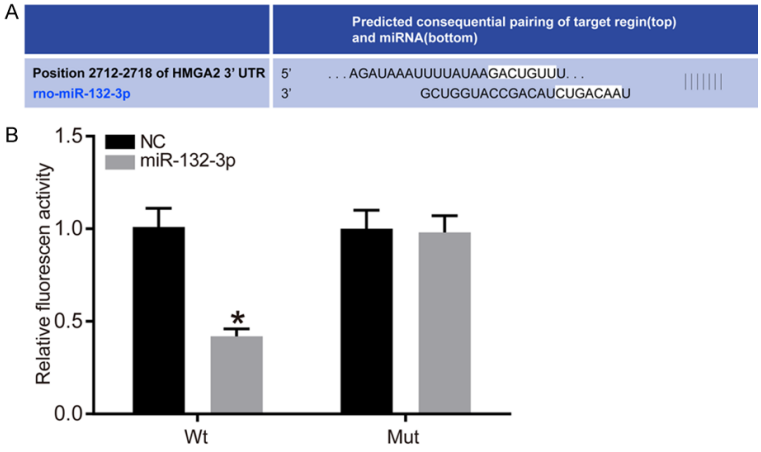

Figure 1. Target relationship between miR-132-3p and HMGA2. A. The predicted binding site of miR-132-3p on HMGA2; B. The results of dual-luciferase reporter gene assay. Compared with NC group, *P < 0.05. HMGA2: high-mobility group AT-hook 2; Wt: wild-type strain (HMGA2-Wt) harboring the luciferase reporter plasmid containing target site in 3'UTR of HMGA2; Mut: luciferase plasmid containing S mutation sequence (HMGA2-Mut).

times for 5 min each time. Then the membrane was incubated with primary antibodies, rabbit anti-mouse HMGA2 (1:1,000; Abcam Company, UK), VEGF (1:1,000; Abcam, UK), BMP-2 (1:1,000; Abcam, UK) and GAPDH (1:1,000; Abcam, UK) overnight at 4°C. The blotting membrane was rinsed with TBST (3 times, 5 min each time) to remove the remaining primary antibodies, and then immersed in secondary antibody, HRP-labeled goat anti-rabbit IgG (1:2,000; Abcam, UK) at room temperature for 1 h. After being rinsed with TBST (3 times, 5 min each time), the membrane was immersed in the reaction solution containing electrogenerated chemiluminescence (ECL) regent (batch number 210452, Bio-Rad Company, United States) at room temperature for 1 min. After pipetting out the reaction solution, the membrane was soaked with an appropriate amount of DAB color-developing filling liquid, sealed in plastic wrap and then exposed to an X-ray film in a dark room. GAPDH was used as internal control, and the amount of target protein was shown by the ratio of target band gray value to the internal control band gray value (Image-Pro plus 6.0, Media Cybernetics, USA).

Statistical analysis

All the data were analyzed using the SPSS 21.0 software (SPSS Inc., Chicago, II, USA). The measurement data were expressed as mean ± standard deviation ($\bar{x}$ ± sd). The comparisons among multiple groups were conducted using one-way analysis of variance, and the difference between two groups was compared by Bonferroni post-hoc test. *P* values < 0.05 were considered statistically significant.

Results

Animal modeling

Of the 100 model rats, 8 rats died after the surgery, and 90 of the survived rats were randomly selected for follow-up experiments. The 90 model rats were randomly divided into six groups: Model group, NC group, miR-132-3p mimic group, miR-132-3p inhibitor group, siRNA-HMGA2 group, and miR-132-3p mimic + siRNA-HMGA2 group, with 15 rats in each group. Rats in all the groups except model group were injected with corresponding complex via caudal vein. The success rate of postoperative modeling was 92.00% (92/100).

Target relationship between miR-132-3p and HMGA2

According to analysis from Targetscan.org, binding site of miR-132-3p on HMGA2 mRNA was identified, and HMGA2 was the target gene of miR-132-3p. Dual-luciferase reporter gene assay showed that compared with NC group, luciferase activity in 3'UTR of wild-type miR-132-3p could be inhibited by miR-132-3p (P < 0.05), while that of mutant miR-132-3p was not inhibited. This indicates that miR-132-3p can specifically bind HMGA2 3'UTR and downregulate HMGA2 gene expression after transcription. See **Figure 1**.

Levels of serum bone markers, P1NP, BAP and OC

At the 2nd, 4th and 8th weeks after modeling, compared with Normal group, serum P1NP, BAP and OC levels in other groups were raised significantly (all P < 0.05). Compared with Model group, serum P1NP, BAP and OC levels in miR-132-3p mimic group, siRNA-HMGA2 group, and miR-132-3p mimic + siRNA-HMGA2 group

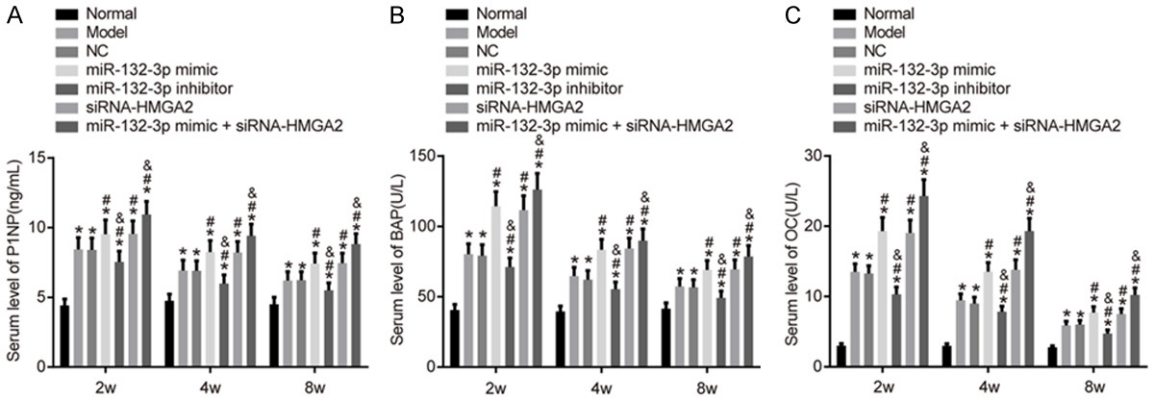

Figure 2. Levels of serum bone markers, P1NP, BAP and OC in rats of all groups. A. Serum level of P1NP of rats in all groups; B. Serum level of BAP of rats in all groups; C. Serum level of OC of rats in all groups. Compared with normal group, $^{*}P < 0.05$; compared with model group, $^{\#}P < 0.05$; compared with miR-132-3p mimic group, $^{\&}P < 0.05$. P1NP: procollagen type 1 N-terminal propeptide; BAP: bone alkaline phosphatase; OC: osteocalcin.

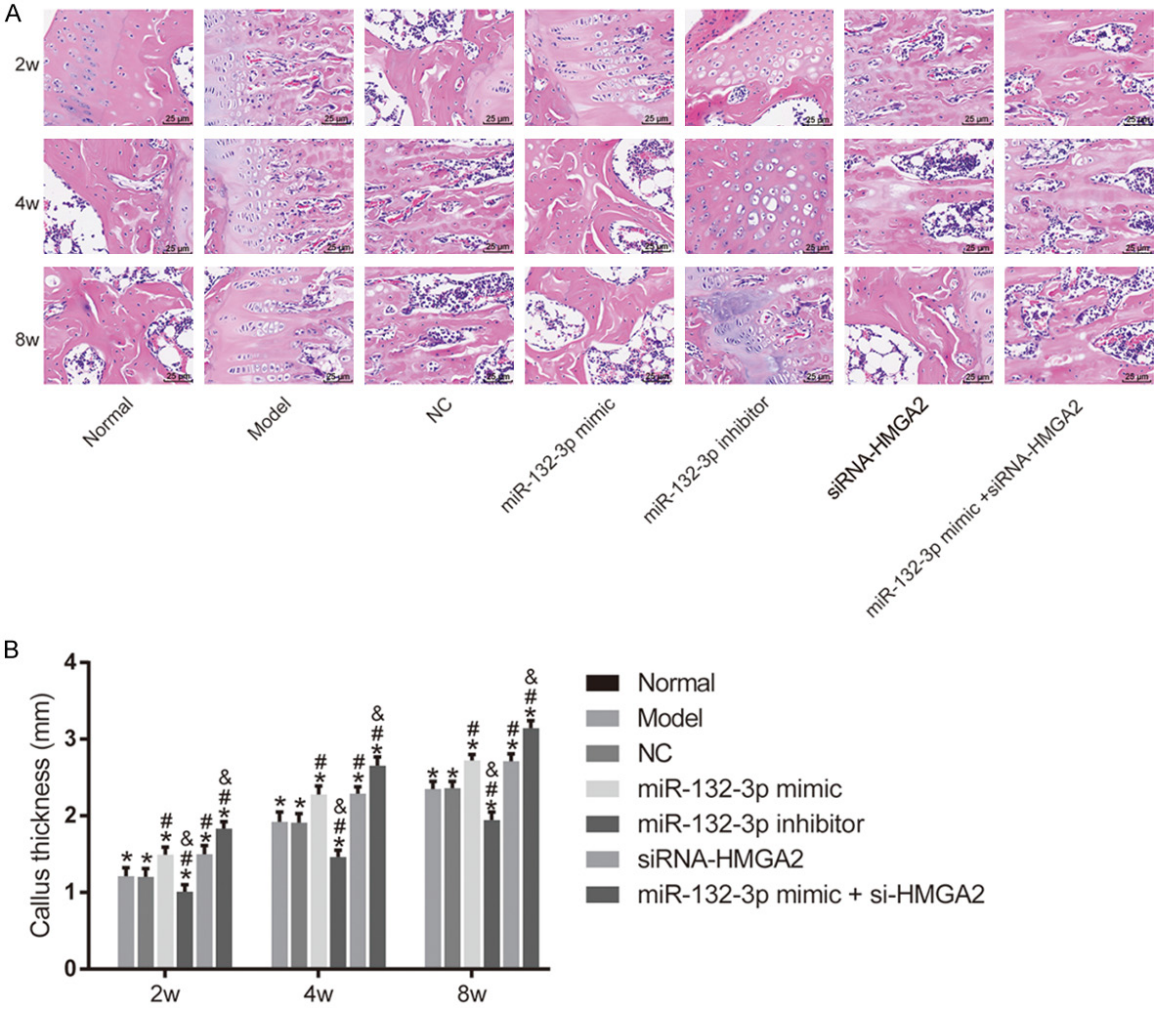

Figure 3. Callus thickness and maturity of femur of rats in all groups observed through HE staining (400×). A. HE staining of femoral tissue; B. Histogram of callus thickness of rats in each group. Compared with normal group, $^{*}P < 0.05$; compared with model group, $^{\#}P < 0.05$; compared with microRNA-132-3p mimic group, $^{\&}P < 0.05$.

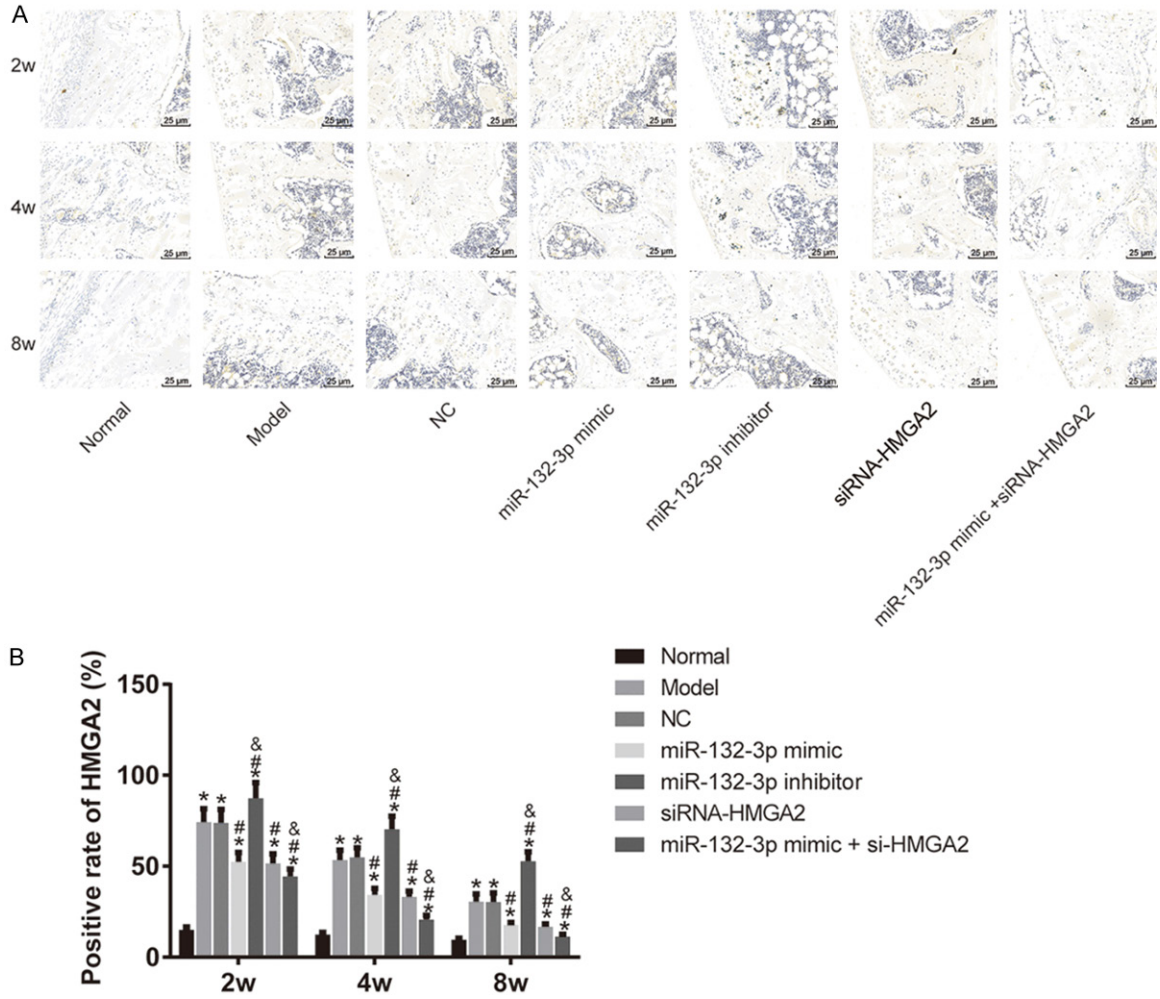

Figure 4. Immunohistochemical results of rats in all groups. A. Microscopic image of immunohistochemical staining (400×); B. Positive expression rate of HMGA2 protein in all groups. Compared with normal group, $^{*}P < 0.05$; compared with model group, $^{\#}P < 0.05$; compared with miR-132-3p mimic group, $^{\&}P < 0.05$. HMGA2: high-mobility group AT-hook 2.

were elevated significantly (all $P < 0.05$), while those in miR-132-3p inhibitor group were significantly decreased (all $P < 0.05$). There were no statistical differences in the levels of the serum bone markers between NC group and Model group (all $P > 0.05$). Compared with miR-132-3p mimic group, serum P1NP, BAP and OC levels in miR-132-3p mimic + siRNA-HMGA2 group were significantly elevated (all $P < 0.05$), and those in mir-132-3p inhibitor group were decreased (all $P < 0.05$). There were no significant differences in the three bone marker levels between siRNA-HMGA2 group and miR-132-3p mimic group (all $P > 0.05$). The serum levels of P1NP, BAP and OC in all the six modeling groups at the 4th and 8th weeks after modeling were significantly lower than those at the 2nd week, and the decrease in the 8th week was more obvious (all $P < 0.05$). See **Figure 2**.

Callus thickness and maturity of rats in each group

Trabeculae, osteoblasts and chondrocytes were abundant in Normal group. At the 2nd week after modeling, trabecular formation was rare in Model group, NC group and miR-132-3p inhibitor group, with more mononuclear macrophages and multinucleated giant cells. The miR-132-3p mimic group, siRNA-HMGA2 group and miR-132-3p mimic + siRNA-HMGA2 group presented more trabeculae, osteoblasts and chondrocytes. At the 4th week, small amount of bone trabeculae and bone cells formed in

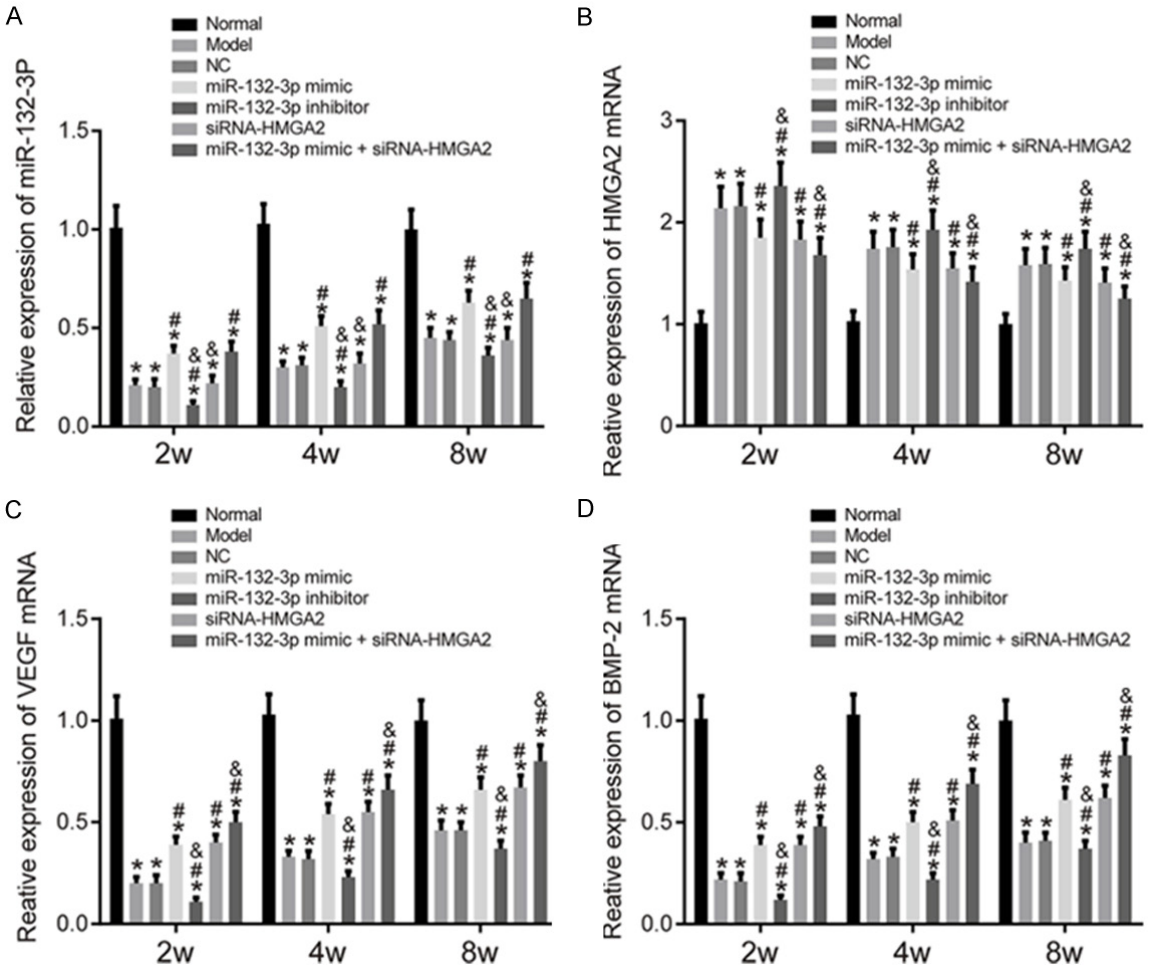

Figure 5. Expression levels of miR-132-3p and microRNAs of HMGA2, VEGF and BMP-2. A. Histogram of miR-132-3p expression of rats in all groups; B. Histogram of HMGA2 mRNA expression of rats in all groups; C. Histogram of VEGF mRNA expression of rats in all groups; D. Histogram of BMP-2 mRNA expression of rats in all groups. Compared with normal group, $^{*}P < 0.05$; compared with model group, $^{\#}P < 0.05$; compared with miR-132-3p mimic group, $^{\&}P < 0.05$. HMGA2: high-mobility group AT-hook 2; VEGF: vascular endothelial growth factor; BMP-2: bone morphogenetic protein-2.

Model group, NC group and miR-132-3p inhibitor group with a low maturity of callus. The trabeculae of miR-132-3p mimic group, siRNA-HMGA2 group and miR-132-3p mimic + siRNA-HMGA2 group began to physically connect with each other, and some trabeculae fused into one piece. At the 8th week, some bone trabeculae fused in Model group, NC group and miR-132-3p inhibitor group with a low maturity of callus. The trabecular bones of miR-132-3p mimic group, siRNA-HMGA2 group and miR-132-3p mimic + siRNA-HMGA2 group were reshaped, and more osteoclasts were observed as well. At the 2nd, 4th and 8th weeks, model group, NC group and microRNA-132-3p inhibitor group were inferior to microRNA-132-3p mimic group, siRNA-HMGA2 group and microRNA-132-3p mimic + siRNA-HMGA2 group in callus thickness (all $P < 0.05$). Furthermore, microRNA-132-3p mimic + siRNA-HMGA2 group was superior to microRNA-132-3p mimic group and siRNA-HMGA2 group in callus thickness (both $P < 0.05$). See **Figure 3**.

Positive expression rate of HMGA2 protein in femur tissue

At the 2nd, 4th and 8th weeks after modeling, compared with Normal group, the positive expression levels of HMGA2 protein in fracture tissues of rats in other 6 groups were increased significantly (all $P < 0.05$). Compared with

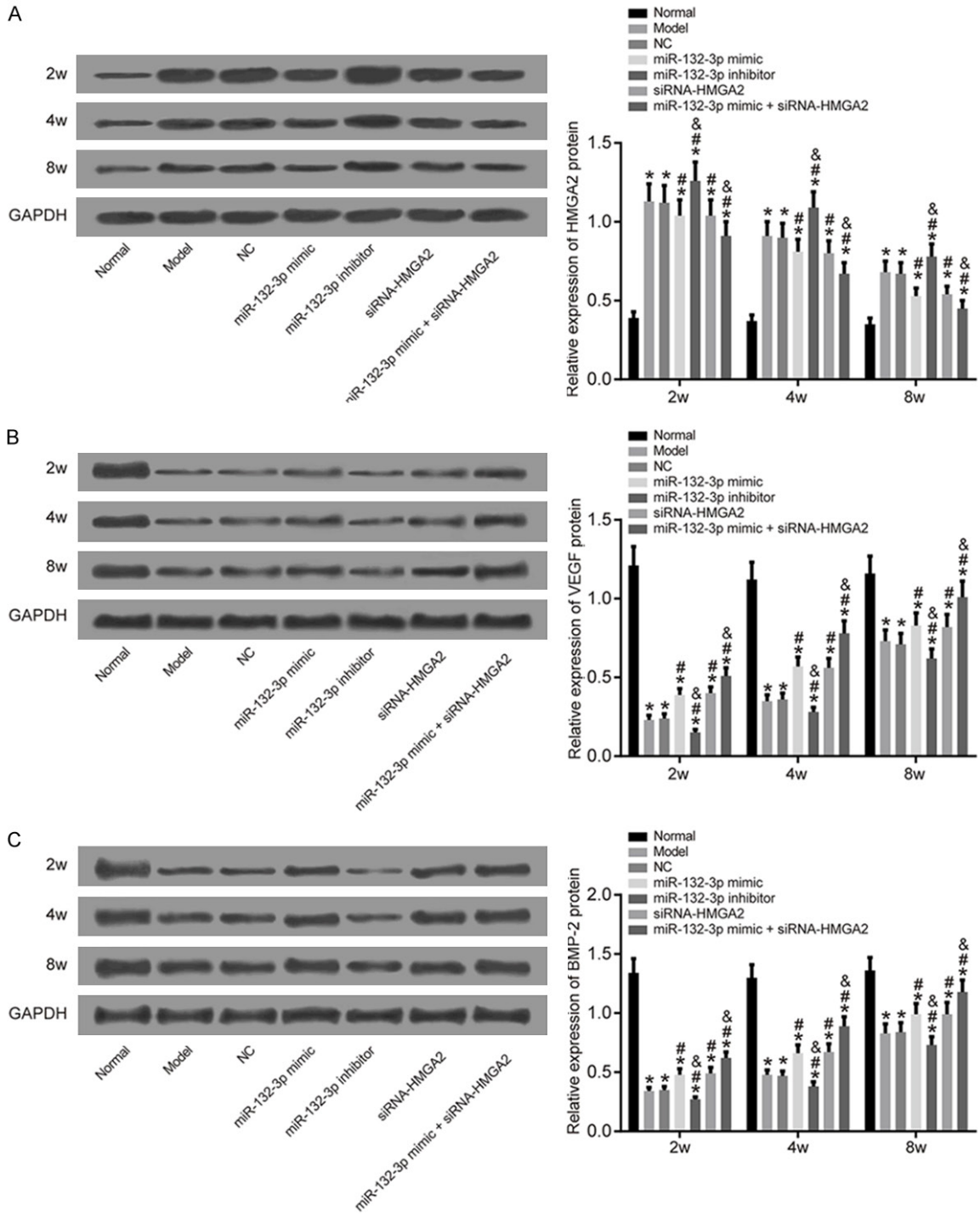

Figure 6. Protein expression levels of HMGA2, VEGF and BMP-2. A. HMGA2 protein imprint and its histogram of rats in all groups; B. VEGF protein imprint and its histogram of rats in all groups; C. BMP-2 protein imprint and its histogram of rats in all groups. Compared with normal group, $^{*}P < 0.05$; compared with model group, $^{\#}P < 0.05$; compared with miR-132-3p mimic group, $^{\&}P < 0.05$. HMGA2: high-mobility group AT-hook 2; VEGF: vascular endothelial growth factor; BMP-2: bone morphogenetic protein-2.

Model group, the levels of HMGA2 protein in fracture tissues of miR-132-3p mimic group, siRNA-HMGA2 group and miR-132-3p mimic + siRNA-HMGA2 group were decreased signifi-

cantly (all P < 0.05). In miR-132-3p inhibitor group, however, there was a significant decline in the positive expression level of HMGA2 protein in fracture tissues (P < 0.05), and there was no significant difference between the model group and NC group (P > 0.05). Compared with miR-132-3p mimic group, the positive expression level of HMGA2 protein in fracture tissues of miR-132-3p mimic + siRNA-HMGA2 group was significantly decreased (P < 0.05), and the level of miR-132-3p inhibitor group was significantly elevated (P < 0.05). There was no significant difference between siRNA-HMGA2 group and miR-132-3p mimic group (P > 0.05). At the 4th and 8th weeks, the positive expression levels of HMGA2 protein in the fracture tissues of rats in groups except Normal group were significantly lower than those at the 2nd week, and the decrease in the 8th week was more obvious (P < 0.05). See **Figure 4**.

MicroRNA expression levels of miR-132-3p, HMGA2, VEGF and BMP-2

At the 2nd, 4th and 8th after modeling, compared with Normal group, the mRNA expression levels of miR-132-3p, VEGF and BMP-2 in other groups were decreased (all P < 0.05), along with increase in the level of HMGA2 (all P < 0.05). Compared with Model group, miR-132-3p mimic group and miR-132-3p mimic + siRNA-HMGA2 group presented increases in miR-132-3p expression level and mRNA expression levels of VEGF and BMP-2, and decrease in mRNA expression level (all P < 0.05). Compared with Model group, siRNA-HMGA2 group presented no difference in miR-132-3p expression level (P > 0.05), but decrease in mRNA expression level of HMGA2, and increases in mRNA expression levels of VEGF and BMP-2 (all P < 0.05). Compared with Model group, miR-132-3p inhibitor group presented decreases in miR-132-3p expression level and mRNA expression levels of VEGF and BMP-2, and increase in mRNA expression level of HMGA2 (all P < 0.05). The differences between Model group and NC group were not significant (all P > 0.05). Compared with miR-132-3p mimic group, siRNA-HMGA2 group presented significant decrease in miR-132-3p expression level (P < 0.05), but with no significant differences in the mRNA expression levels of HMGA2, VEGF and BMP-2 (all P > 0.05). Compared with miR-132-3p mimic group, miR-13-2-3p mimic + siRNA-HMGA2 group presented significant decrease in HMGA2 expression level (P<0.05), and significant increases in mRNA expression levels of VEGF and BMP-2 (all P < 0.05), but with no significant difference in miR-132-3p expression level (P > 0.05). Compared with miR-132-3p mimic group, miR-132-3p inhibitor group presented decreases in miR-132-3p expression level and mRNA expression levels of VEGF and BMP-2, and increase in mRNA expression level of HMGA2 (all P < 0.05). Compared with the 2nd week, all the six modeling groups, at the 4th and 8th weeks, showed increases in miR-132-3p expression level and mRNA expression levels of VEGF and BMP-2, and decrease in mRNA expression level of HMGA2 (all P < 0.05), and the decrease or increase in the 8th week was more obvious (all P < 0.05). See **Figure 5**.

Protein expression levels of HMGA2, VEGF and BMP-2

Compared with Normal group, at the 2nd, 4th and 8th weeks after modeling, protein expression level of HMGA2 in other groups was elevated, while the protein expression levels of VEGF and BMP-2 were both decreased (all P < 0.05). Compared with Model group, HMGA2 protein expression levels in miR-132-3p mimic group, siRNA-HMGA2 group and miR-132-3p mimic + siRNA-HMGA2 group were decreased, while VEGF and BMP-2 protein expression levels were both increased (all P < 0.05). While in the miR-132-3p inhibitor group, the results were quite the opposite. There were no significant differences between Model group and NC group (all P > 0.05). There were no significant differences in protein expression levels of HMGA2, VEGF and BMP-2 between siRNA-HMGA2 group and miR-132-3p mimic group (all P > 0.05). Compared with miR-132-3p mimic group, protein expression level of HMGA2 in miR-132-3p mimic + siRNA-HMGA2 group was significantly decreased (P < 0.05), while the protein expression levels of VEGF and BMP-2 were both significantly increased, and mir-132-3p inhibitor group had the opposite results (all P < 0.05). Compared with the 2nd week, at the 4th and 8th weeks, the protein expression levels of all the six modeling groups were decreased, while the protein expression levels of VEGF and BMP-2 were both increased (all P < 0.05), and the decrease or increase at the 8th week was more obvious (all P < 0.05). See **Figure 6**.

Discussion

Fracture healing is a spontaneous self-repair process. Despite the strong regenerative ability of bones, fracture nonunion rate is still as high as 5-10%. According to statistics, there are nearly 70 million osteoporosis patients existing in China. Traditional methods for fracture treatment require long-time healing with relatively poor effect. Therefore, it is necessary to find an efficient and alternative modality for fracture healing.

Initially, through analysis by Targetscan.org, a binding site between miR-132-3p and high-mobility group AT-hook 2 (HMGA2) was found, that is, HMGA2, which is the target gene of miR-132-3p. A previous study has found that miR-132-3p plays a negative regulatory role in osteogenic differentiation by affecting acetylation and protein activity [18]. HMGA2, belonging to the high mobility group protein A (HMGA) family, can not only activate or inhibit the activity of transcription factors to regulate the transcription of certain genes, but also maintain the differentiation potential and self-renewal ability of stem cells and participate in the regulation process of multiple biological events [19]. A study reported that HMGA2 was highly expressed in embryonic tissues and malignant tumors, and its higher expression indicates the lower survival rate of the patients [20]. In this study, it was found that miR-132-3p could downregulate HMGA2 gene expression after binding to specific sites in 3'UTR of HMGA2 gene.

Afterwards, it was found that the targeting inhibition of HMGA2 expression by miR-132-3p activates VEGF pathway. As everyone knows, VEGF is the most potent and specific angiogenic factor at present; angiogenesis plays an important role in osteogenesis, bone regeneration and repair, and serves as an important link in the process of fracture healing [21, 22]. HMGA2 indirectly regulates the expression of VEGF and other proteins by enhancing the activity of transcription factor AP1 complex and increasing the binding affinity of AP1 to Etal family proteins. The VEGF pathway is one of the many signaling pathways that HMGA2 participates in biological processes in vivo [23]. VEGF promotes vascular endothelial cell proliferation and angiogenesis by binding with specific receptors on vascular endothelial cells, thus providing oxygen and nutrients to fracture segments, and transporting metabolites, as well as providing a microenvironment necessary for bone regeneration [24]. Meanwhile, VEGF also participates in callus transformation and other links. The expression levels of VEGF mRNA and protein are gradually elevated with time during the healing process [25]. In this study, compared with the 2nd week after fracture modeling, the mRNA and protein expression levels of VEGF and BMP-2 in model group, NC group, miR-132-3p mimic group, miR-132-3p inhibitor group, siRNA-HMGA2 group and miR-132-3p mimic + siRNA-HMGA2 group were all elevated at the 4th and 8th weeks, which was consistent with the aforementioned findings. Here, BMP is an induced osteogenic factor, which plays an important role in the formation and differentiation of bones and cartilages. Together with VEGF, BMP is usually considered to be an important factor in promoting osteogenesis [26]. The results in this study showed that the expression of HMGA2 was negatively correlated with the expression of VEGF. Inhibition of HMGA2 might activate the expression of VEGF through different pathways, and VEGF's expression could promote the formation of new blood vessels, thus leading to the enhancement of bone regeneration and repair ability.

Moreover, after miR-132-3p targeting HMGA2 and activating VEGF pathway, the levels of bone markers like P1NP, BAP and OC are improved. P1NP reflects the deposition of type I collagen in the blood, and its concentration serves as a specific indicator reflecting osteoblast activity and bone formation within a certain range [27]. BAP directly reflects the activity or functional status of osteoblasts and is one of the recognized markers of bone formation [28]. OC, synthesized and secreted by osteoblasts, is the main and the most abundant non-collagenous protein in human bone, functioning as an indicator of bone metabolism; and its concentration can directly reflect osteoblast activity and bone formation [29].

In summary, the targeting inhibition of HMGA2 expression by miR-132-3p can activate VEGF pathway and thus accelerate angiogenesis in fracture sites. miR-132-3p plays a vital role in inducing activation of VEGF pathway, and can be regarded as an important factor involved in fracture healing, which brings up a new idea for

fracture treatment. However, this study was carried out on the rat models, and whether miR-132-3p is suitable for human requires further research. Moreover, the role of miR-132-3p and its targeted gene, HMGA2, in fracture healing is studied for the first time. So, it is hard to compare the results with the findings in other studies, and there is also a lack of strong evidence existing from relevant studies. Additionally, due to easy recurrence of fracture and its complexity in healing, multiple targets can be taken into account to improve fracture healing when establishing a treatment protocol. Either way, we still need to continue exploring the methods for treating bone fracture.

Disclosure of conflict of interest

None.

Address correspondence to: Weiguo Liang, Department of Orthopedics, Guangzhou Red Cross Hospital, Medical College, Ji'nan University, No. 396 Tongfu Middle Road, Guangzhou 510220, Guangdong Province, China. Tel: +86-020-84412233; Fax: +86-020-84412233; E-mail: liangweiguo10gz@163.com

References

[1] Anderson TL. Fracture mechanics: fundamentals and applications Surjya Kumar Maiti. Mrs Bull 2016; 41: 635-636.

[2] Cheung WH, Miclau T, Chow SK, Yang FF and Alt V. Fracture healing in osteoporotic bone. Injury 2016; 47 Suppl 2: S21-S26.

[3] Waki T, Lee SY, Niikura T, Iwakura T, Dogaki Y, Okumachi E, Oe K, Kuroda R and Kurosaka M. Profiling microRNA expression during fracture healing. BMC Musculoskelet Disord 2016; 17: 83.

[4] Gibbs DM, Black CR, Dawson JI and Oreffo RO. A review of hydrogel use in fracture healing and bone regeneration. J Tissue Eng Regen Med 2016; 10: 187-198.

[5] Kostenuik P and Mirza FM. Fracture healing physiology and the quest for therapies for delayed healing and nonunion. J Orthop Res 2017; 35: 213-223.

[6] Neagu TP, Tiglis M, Cocolos I and Jecan CR. The relationship between periosteum and fracture healing. Rom J Morphol Embryol 2016; 57: 1215-1220.

[7] Rupaimoole R and Slack FJ. MicroRNA therapeutics: towards a new era for the management of cancer and other diseases. Nat Rev Drug Discov 2017; 16: 203-222.

[8] Thomson DW and Dinger ME. Endogenous microRNA sponges: evidence and controversy. Nat Rev Genet 2016; 17: 272-283.

[9] Luzi E, Marini F, Sala SC, Tognarini I, Galli G and Brandi ML. Osteogenic differentiation of human adipose tissue-derived stem cells is modulated by the miR-26a targeting of the SMAD1 transcription factor. J Bone Miner Res 2008; 23: 287-295.

[10] Li ZY, Hassan MQ, Volinia S, van Wijnen AJ, Stein JL, Croce CM, Lian JB and Stein GS. A microRNA signature for a BMP2-induced osteoblast lineage commitment program. Proc Natl Acad Sci U S A 2008; 105: 13906-13911.

[11] Schaap-Oziemlak AM, Raymakers RA, Bergevoet SM, Gilissen C, Jansen BJ, Adema GJ, Kögler G, Sage CL, Agami R, van der Reijden BA and Jansen JH. MicroRNA hsa-miR-135b regulates mineralization in osteogenic differentiation of human unrestricted somatic stem cells. Stem Cells Dev 2010; 19: 877-885.

[12] Itoh T, Nozawa Y and Akao Y. MicroRNA-141 and -200a are involved in bone morphogenetic protein-2-induced mouse pre-osteoblast differentiation by targeting distal-less homeobox 5. J Biol Chem 2009; 284: 19272-19279.

[13] Jasinska M, Milek J, Cymerman IA, Leski S, Kaczmarek L and Dziembowska M. miR-132 regulates dendritic spine structure by direct targeting of matrix metalloproteinase 9 mRNA. Mol Neurobiol 2016; 53: 4701-4712.

[14] Karakas M, Schulte C, Appelbaum S, Ojeda F, Lackner KJ, Munzel T, Schnabel RB, Blankenberg S and Zeller T. Circulating microRNAs strongly predict cardiovascular death in patients with coronary artery disease-results from the large AtheroGene study. Eur Heart J 2017; 38: 516-523.

[15] Zucker S, Mirza H, Conner CE, Lorenz AF, Drews MH, Bahou WF and Jesty J. Vascular endothelial growth factor induces tissue factor and matrix metalloproteinase production in endothelial cells: conversion of prothrombin to thrombin results in progelatinase A activation and cell proliferation. Int J Cancer 1998; 75: 780-786.

[16] Zeng ZH, Yu L, Gong LL, Xiao X and Zeng J. Expression of BMP-2 and VEGF in healing of fracture. Med J Wuhan Univ 2005; 26: 467-469+552.

[17] Okazaki K, Jingushi S, Ikenoue T, Urabe K, Sakai H and Iwamoto Y. Expression of parathyroid hormone-related peptide and insulin-like growth factor I during rat fracture healing. J Orthop Res 2003; 21: 511-520.

[18] Hu ZB, Wang YX, Sun ZY, Wang H, Zhou H, Zhang LC, Zhang S and Cao XS. miRNA-132-3p inhibits osteoblast differentiation by targeting

Ep300 in simulated microgravity. Sci Rep 2015; 5: 18655.
[19] Zhao XP, Zhang H, Jiao JY, Tang DX, Wu YL and Pan CB. Overexpression of HMGA2 promotes tongue cancer metastasis through EMT pathway. J Transl Med 2016; 14: 26.
[20] Pallante P, Sepe R, Puca F and Fusco A. High mobility group a proteins as tumor markers. Front Med 2015; 2: 15.
[21] Lockhart AC, Rothenberg ML, Dupont J, Cooper W, Chevalier P, Sternas L, Buzenet G, Koehler E, Sosman JA, Schwartz LH, Gultekin DH, Koutcher JA, Donnelly EF, Andal R, Dancy I, Spriggs DR and Tew WP. Phase I study of intravenous vascular endothelial growth factor trap, aflibercept, in patients with advanced solid tumors. J Clin Oncol 2010; 28: 207-214.
[22] Oshima Y, Deering T, Oshima S, Nambu H, Reddy PS, Kaleko M, Connelly S, Hackett SF and Campochiaro PA. Angiopoietin-2 enhances retinal vessel sensitivity to vascular endothelial growth factor. J Cell Physiol 2004; 199: 412-417.
[23] Silveira LH, Martinez-Lavin M, Pineda C, Fonseca MC, Navarro C and Nava A. Vascular endothelial growth factor and hypertrophic osteoarthropathy. Clin Exp Rheumatol 2000; 18: 57-62.
[24] Zha L, Wang ZW, Tang WX, Zhang N, Liao G and Huang Z. Genome-wide analysis of HMGA2 transcription factor binding sites by ChIP on chip in gastric carcinoma cells. Mol Cell Biochem 2012; 364: 243-251.
[25] Athanasopoulos AN, Schneider D, Keiper T, Alt V, Pendurthi UR, Liegibel UM, Sommer U, Nawroth PP, Kasperk C and Chavakis T. Vascular endothelial growth factor (VEGF)-induced up-regulation of CCN1 in osteoblasts mediates proangiogenic activities in endothelial cells and promotes fracture healing. J Biol Chem 2007; 282: 26746-26753.
[26] Lin SJ, Lerch TF, Cook RW, Jardetzky TS and Woodruff TK. The structural basis of TGF-beta, bone morphogenetic protein, and activin ligand binding. Reproduction 2006; 132: 179-190.
[27] Nikahval B, Nazifi S, Heidari F and Khafi MSA. Evaluation of the changes of P1NP and CTX in synovial fluid and blood serum of dogs with experimental osteoarthritis. Comp Clin Pathol 2016; 25: 559-563.
[28] Hamidieh AA, Hamidi Z, Behfar M, Pajouhi Z, Alimoghaddam K, Mohseni F, Ghavamzadeh A, Sobhani M, Larijani B and Mohajeri Tehrani MR. How is the relation between endocrine changes and bone markers in pediatric thalassemic patients after hematopoietic stem cell transplantation. Minerva Pediatr 2016. [Epub ahead of print].
[29] Li JQ, Zhang HY, Yang C, Li YH and Dai ZQ. An overview of osteocalcin progress. J Bone Miner Metab 2016; 34: 367-379.